Electronic Supplementary Material (ESI) for Dalton Transactions.

Supporting Information

Linker Conformation Induced Metal-Organic Framework with high Stability and Efficient Upgrading of Natural Gas

Shi-Ming Li, Hong-Chan Jiang, Qing-Ling Ni, Liu-Cheng Gui, Xiu-Jian Wang**

[a] School of Chemistry and Pharmaceutical Sciences, Guangxi Normal University, Guilin 541004, China.

Table of contents

GNU-1 at 298 K.

Figure S13. Single-site Langmuir-Freundlich model for CH_4 adsorption isotherm on **GNU-1** at 273 K.

References

S1. Supplementary methods

1. Fitting of unary isotherm data

The unary isotherms for CH_4, C_2H_6, and C_3H_8 measured at two different temperatures 273 K, and 298 K in **GNU-1a** were fitted with excellent accuracy using the dual-site Langmuir-Freundlich model, where we distinguish two distinct adsorption sites A and B:

$$q = \frac{q_{sat,A} b_A p^{vA}}{1 + b_A p^{vA}} + \frac{q_{sat,B} b_B p^{vB}}{1 + b_B p^{vB}} \qquad (S1)$$

In eq. (S1), the Langmuir-Freundlich parameters $\boldsymbol{b_A}$ and $\boldsymbol{b_B}$ are both temperature dependent:

$$b_A = b_{A0}\exp\left(\frac{E_A}{RT}\right);\ b_B = b_{B0}\exp\left(\frac{E_B}{RT}\right) \qquad (S2)$$

In eq (S2), $\boldsymbol{E_A}$ and $\boldsymbol{E_B}$ are the energy parameters associated with sites A, and B, respectively.

The unary isotherm fit parameters for each of the guest molecules in **GNU-1a** are provided in Table S2.

2. Isosteric heat of adsorption calculations

The isosteric heat of adsorption ($\boldsymbol{Q_{st}}$) is defined as:

$$Q_{st} = -RT^2\left(\frac{\partial lnp}{\partial T}\right) \qquad (S3)$$

Where the derivative in the right member of eq (S3) is determined at constant adsorbate loading, **q**; the derivative can be determined analytically using equations (S1), (S2), and (S3).

3. IAST calculations of selectivity

The adsorption selectivity for separation for components 1 and 2 is defined by:

$$S_{ads} = \frac{q_1/q_2}{p_1/p_2} \qquad (S4)$$

IAST calculations were carried out for equimolar $C_3H_6/C_3H_8/C_2H_2/C_2H_4/C_2H_6/CH_4$ mixtures at 298 K.

4. Grand canonical monte carlo simulations

All simulations were performed by the Materials Studio (MS) 2020 package. The preferred sorption locations were performed by GCMC simulations with Adsorption fixed pressure task and Metropolis method in the sorption calculation module at 298 K and 1 bar. As for all of the GCMC simulations, the framework was considered to be rigid. The framework and gas molecule were described by the force filed of COMPASSIII. The cutoff radius was set to 12.5 Å, for the Lennard-Jones (LJ) interactions, and the electrostatic interactions, and the Ewald summation method was selected to calculate the electrostatic interactions between adsorbates as well as between adsorbates and the framework. For state point in GCMC simulation, the system adopted 1×10^6 Monte Carlo steps to guarantee equilibration, and the ultimate data was collected for another 1×10^7 Monte Carlo steps. The embedded charges of the atoms of both gas molecules and the framework were assigned by the force filed of COMPASSIII [1].

5. Synthesis of ligand H_6bmipia

Dimethyl 5-amino-phthalate (209 mg, 1 mmol), dimethyl 5-bromomethyl phthalate (631.4 mg, 2.2 mmol) and sodium hydroxide (88 mg, 2.2 mmol) were added into a 250 mL round-bottom flask, and then 50 mL distilled water was added. The reaction was refluxing at 80 °C for 24 h before filtration. Then, the dry white filter cake was transferred to the round-bottom flask, followed, sodium hydroxide and 50 mL distilled water were added into the flask, the reaction was also refluxing at 80 °C for 24 h. Then reaction mixture was poured into the beaker and hydrochloric acid was added, to adjust the pH to 1-2. The yellow solid product was obtained after filtration and drying (800 mg, 81.0 %).

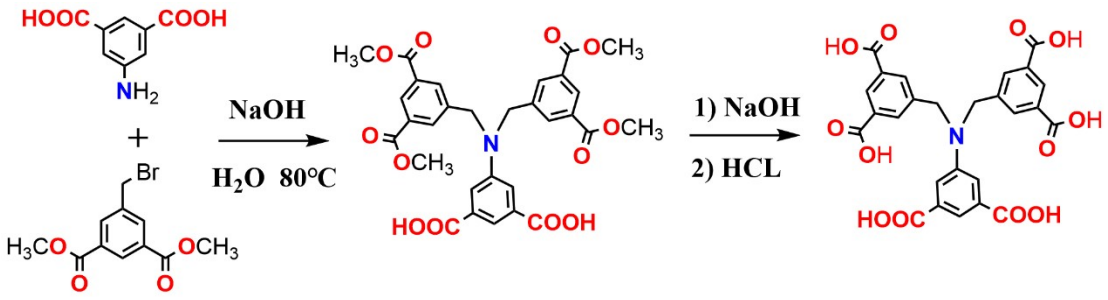

Scheme S1. Synthetic route to the organic linker

S2. Supplementary tables

Table S1. Crystal data and structure refinement parameters for **GNU-1**

Empirical formula	$C_{26}\ H_{19}\ Cu_3\ N\ O_{15}$
Formula weight (g mol^{-1})	776.04
Crystal system	orthorhombic
Space group	Cmce
a (Å)	13.7215(3)
b (Å)	35.1471(8)
c (Å)	19.2775(5)
α/°	90
β(°)	90
γ/°	90
V ($Å^3$)	9297.0(4)
Z	8
ρ_{calc} (g cm^{-3})	1.109
μ (mm^{-1})	2.022
F (000)	3112.0
2Θ range for data collection/°	5.028 to 127.99
Index ranges	-15≤h≤6, -40≤k≤40, -22≤l≤22
Reflections collected	14985
Independent reflections	4018 [R_{int} = 0.0485, R_{sigma} = 0.0303]
Goodness-of-fit on F^2	1.110
Final R indexes [I>=2σ (I)][a]	R_1 = 0.0788, wR_2 = 0.2738
Final R indexes [all data][b]	R_1 = 0.0872, wR_2 = 0.2857
Largest diff. peak/hole / e $Å^{-3}$	0.85/-0.59
CCDC deposition number	2233603

[a] $R_1 = \sum||F_o| - |F_c||/\sum|F_o|$. [b] $wR_2 = \{\sum[w(F_o^2 - F_c^2)^2]/\sum w(F_o^2)^2\}^{1/2}$

Table S2 Comparison of $C_3H_8/C_2H_6/CH_4$ uptakes and C_3H_8/CH_4 (5/85) and C_2H_6/CH_4 (10/85)

selectivities of some reported materials (298 K, 1 bar)

Materials	$C_3H_8/C_2H_6/CH_4$ uptake (mmol/g)	C_3H_8/CH_4 selectivity	C_2H_6/CH_4 selectivity	Reference
$Ni(tmbdc)(dabco)_{0.5}$	5.54/5.81/1.50	274	29	2
FIR-51	4.54/4.21/0.644	326.8	15	3
GNU-1	6.64/4.60/1.12	330.13	17.54	This work
Cu-MOF	5.98/3.22/0.39	203.6	9.3	4
$Fe_{2(}$dobdc)	5.73/5.05/0.792	-	32	5
PAF-40-Fe	2.61/1.87/0.644	56	16.2	6
JUC-100	6.14/4.14/0.479	65	8	7
RT-MIL-100(Fe)	6.85/2.23/3.96	33.3	6	8
HKUST-1	7.13/5.63/0.990	97	17	9
0.3Gly@HKUST-1	7.87/6.55/1.04	173	12.6	9
MIL-142A	5.32/3.82/0.54	1300	13.7	10
BSF-2	2.23/1.46/0.40	2609	53	11
PCN-224	8.25/2.93/0.48	609	12	12
MFM-202a	6.76/4.21/0.45	87	10	13
FJI-C1	6.33/3.72/0.43	471	22	14
UTSA-35a	2.97/2.43/0.43	80	15	15
Zr-FUM	2.38/-/0.53	292	-	16
FIR-7a-ht	7.24/4.06/0.46	78.8	14.6	17
A-AC-4	11.76/6.59/1.18	88.8	15.1	18
JLU-Liu45	3.79/3.78/0.69	42.7	20.1	19
Zr-SDBA	2.42/2.08/0.57	97.5	15.0	19
Zr-OBBA	0.78/0.5/0.16	105.6	16.7	19
UPC-33	4.18/1.56/0.31	41.8	6.64	20
FJI-H21	3.61/3.45/0.32	145.2	17.1	21
UPC-100-In	5.31/5.33/0.51	186.4	17.90	22
LIFM-26	5.21/4.61/0.49	46	11	23

S3. Supplementary figures

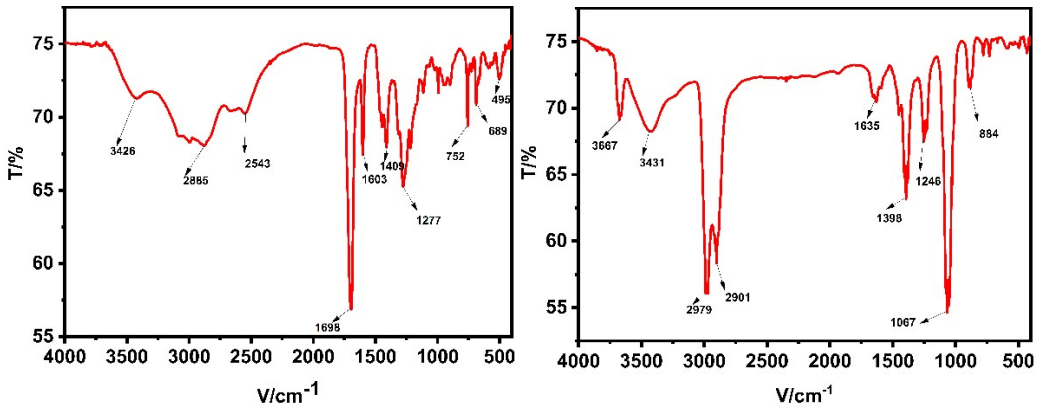

Figure S1. Comparison of FTIR spectra of ligands (left) and as-synthesized **GNU-1** (right).

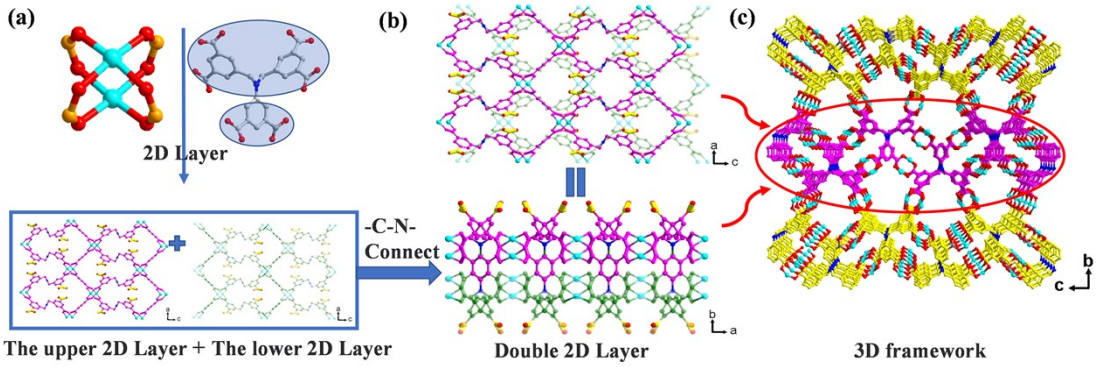

Figure S2. (a) Copper paddlewheel and ligand construct 2D Layer; (b) The Double 2D layer; (c) 3D framework.

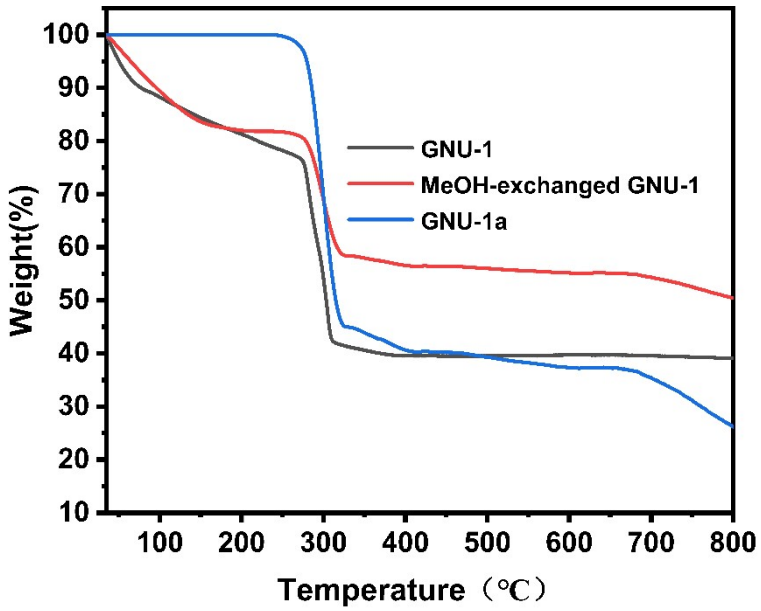

Figure S3. TGA curves of as-synthesized, MeOH-exchanged, and activated **GNU-1** under N_2 atmosphere.

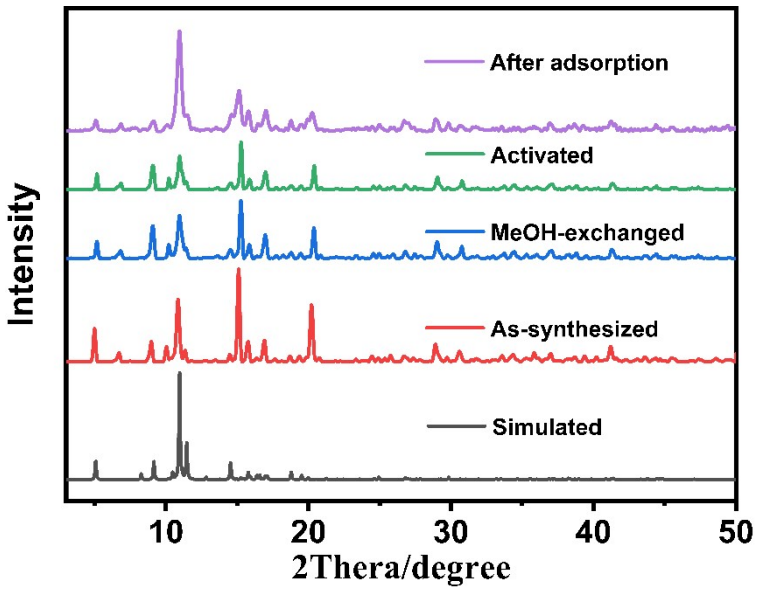

Figure S4. Comparison of PXRD patterns of **GNU-1**.

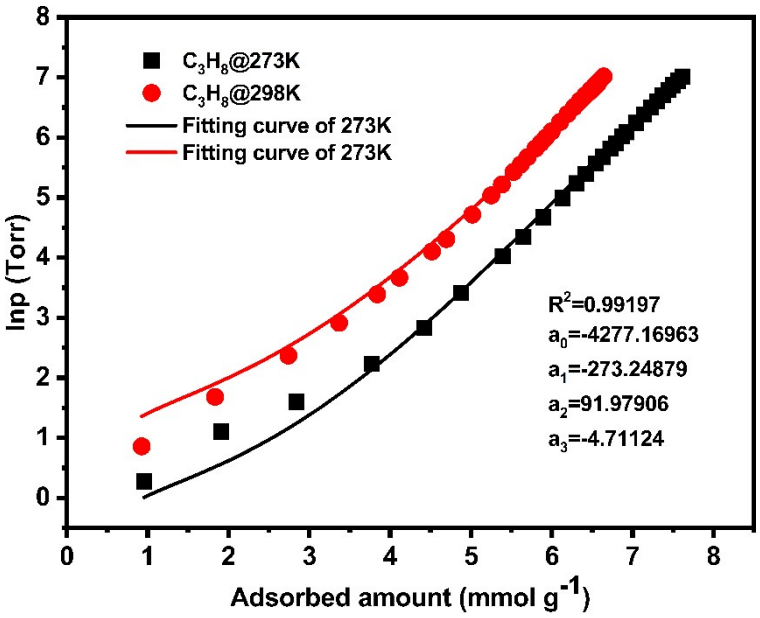

Figure S5 Virial fitting of C_3H_8 adsorption data for **GNU-1** at 273 and 298 K.

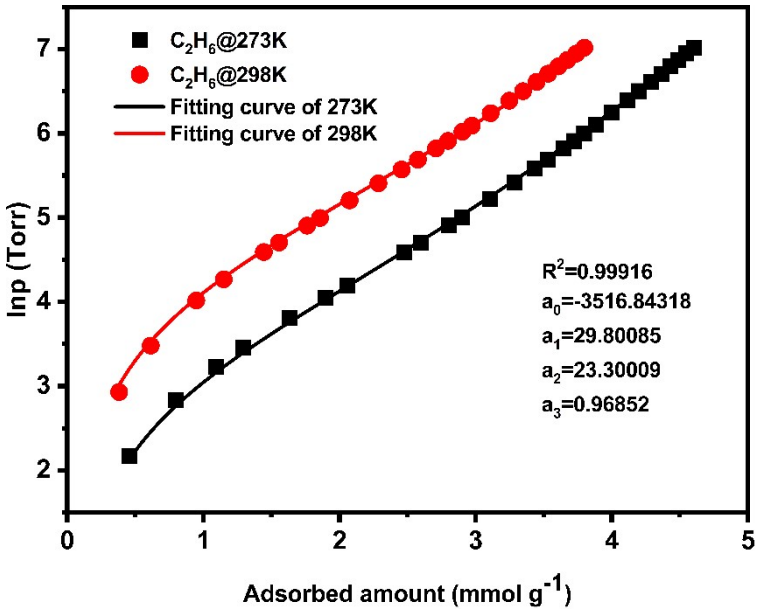

Figure S6 Virial fitting of C_2H_6 adsorption data for **GNU-1** at 273 and 298 K.

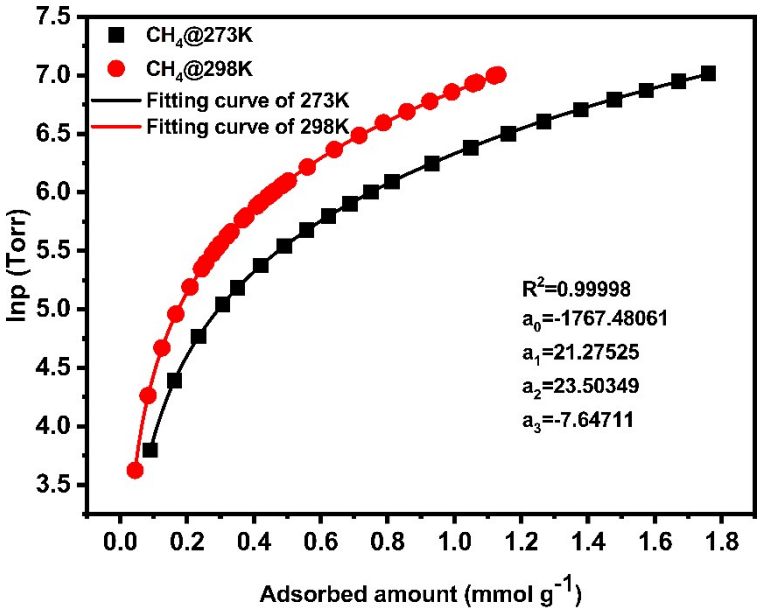

Figure S7 Virial fitting of CH_4 adsorption data for **GNU-1** at 273 and 298 K.

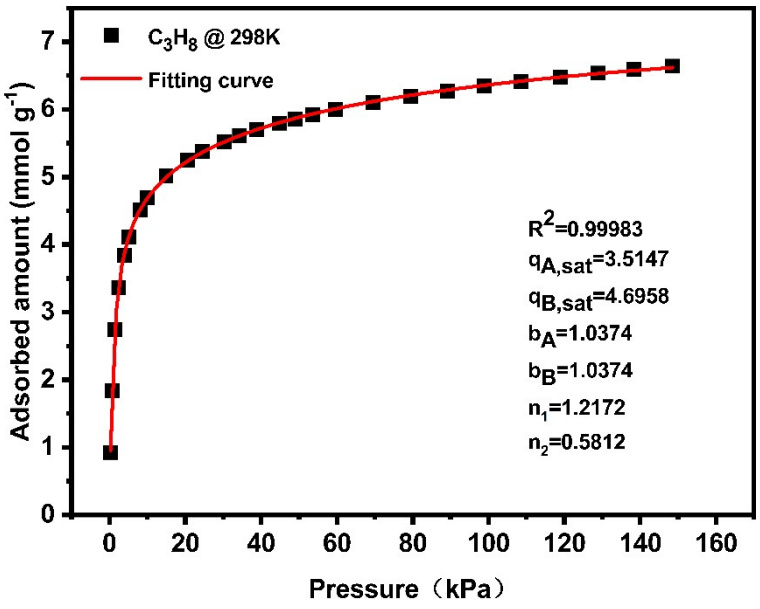

Figure S8 Dual-site Langmuir-Freundlich model for C_3H_8 adsorption isotherm on **GNU-1** at 298 K.

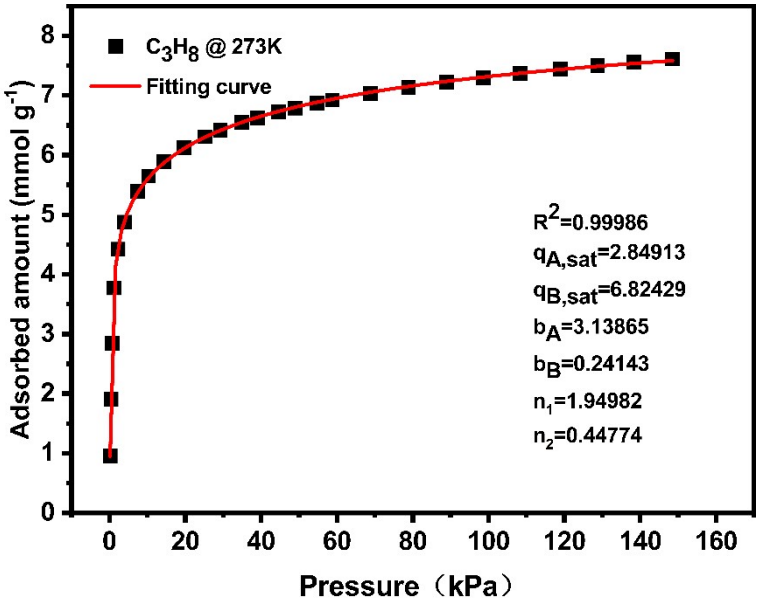

Figure S9 Dual-site Langmuir-Freundlich model for C_3H_8 adsorption isotherm on **GNU-1** at 273 K.

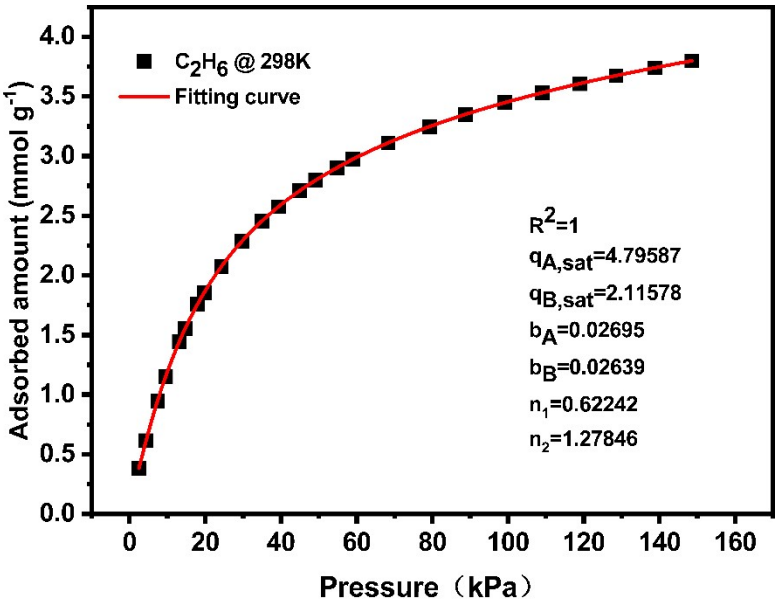

Figure S10 Dual-site Langmuir-Freundlich model for C_2H_6 adsorption isotherm on **GNU-1** at 298 K.

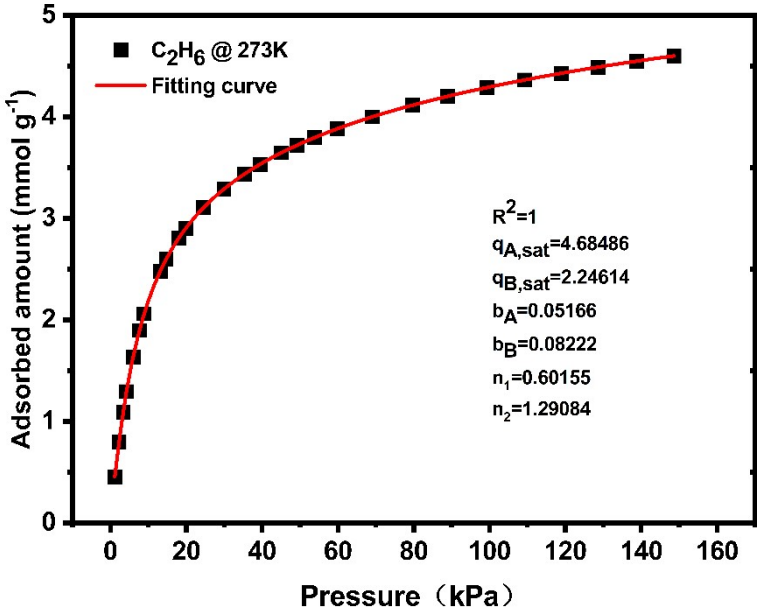

Figure S11 Dual-site Langmuir-Freundlich model for C_2H_6 adsorption isotherm on **GNU-1** at 273 K.

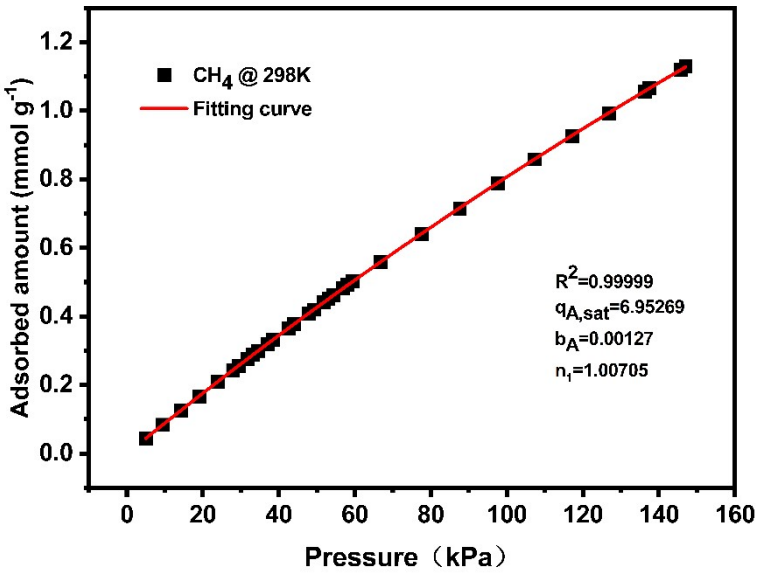

Figure S12 Single-site Langmuir-Freundlich model for CH_4 adsorption isotherm on **GNU-1** at 298 K.

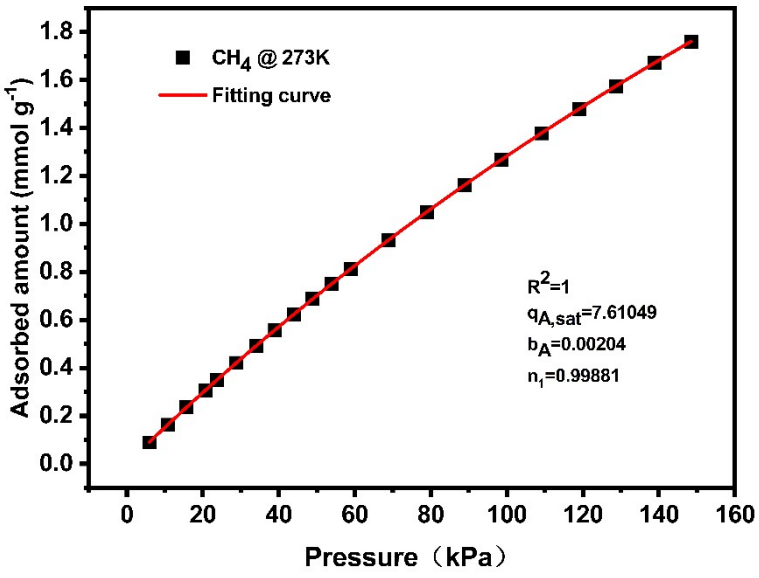

Figure S13 Single-site Langmuir-Freundlich model for CH_4 adsorption isotherm on **GNU-1** at 273 K.

References

1. N. Metropolis, A. W. Rosenbluth, M. N. Rosenbluth, A. H. Teller and E. Teller, Equation of State Calculations by Fast Computing Machines, *The Journal of Chemical Physics*, 1953, **21**, 1087-1092.
2. Y. Wu, Z. Liu, J. Peng, X. Wang, X. Zhou and Z. Li, Enhancing Selective Adsorption in a Robust Pillared-Layer Metal–Organic Framework via Channel Methylation for the Recovery of C2–C3 from Natural Gas, *ACS Appl. Mater. Interfaces*, 2020, **12**, 51499-51505.
3. H. R. Fu, F. Wang and J. Zhang, A stable zinc-4-carboxypyrazole framework with high uptake and selectivity of light hydrocarbons, *Dalton Trans*, 2015, **44**, 2893-2896.
4. S.-M. Wang and Q.-Y. Yang, A copper-based metal-organic framework for upgrading natural gas

through the recovery of C_2H_6 and C_3H_8, *Green Chemical Engineering*, 2022, **4**(1): 81-87.
5. E. D. Bloch, R. Krishna and J. R. Long, Hydrocarbon Separations in a Metal-Organic Framework with Open Iron(II) Coordination Sites, *science*, 2012, **335**(6076): 1606-1610.
6. S. Meng, H. Ma, L. Jiang, H. Ren and G. Zhu, A facile approach to prepare porphyrinic porous aromatic frameworks for small hydrocarbon separation, *J. Mater. Chem. A*, 2014, **2**, 14536-14541.
7. J. Jia, L. Wang, F. Sun, X. Jing, Z. Bian, L. Gao, R. Krishna and G. Zhu, The adsorption and simulated separation of light hydrocarbons in isoreticular metal-organic frameworks based on dendritic ligands with different aliphatic side chains, *Chemistry*, 2014, **20**, 9073-9080.
8. B. Yuan, X. Wang, X. Zhou, J. Xiao and Z. Li, Novel room-temperature synthesis of MIL-100(Fe) and its excellent adsorption performances for separation of light hydrocarbons, *Chemical Engineering Journal*, 2019, **355**, 679-686.
9. Y. Wu, Y. Sun, J. Xiao, X. Wang and Z. Li, Glycine-Modified HKUST-1 with Simultaneously Enhanced Moisture Stability and Improved Adsorption for Light Hydrocarbons Separation, *ACS Sustainable Chemistry & Engineering*, 2018, **7**, 1557-1563.
10. Y. Yuan, H. Wu, Y. Xu, D. Lv, S. Tu, Y. Wu, Z. Li and Q. Xia, Selective extraction of methane from C1/C2/C3 on moisture-resistant MIL-142A with interpenetrated networks, *Chemical Engineering Journal*, 2020, **395**.125057.
11. Y. Zhang, L. Yang, L. Wang, S. Duttwyler and H. Xing, A Microporous Metal-Organic Framework Supramolecularly Assembled from a Cu(II) Dodecaborate Cluster Complex for Selective Gas Separation, *Angew Chem Int Ed Engl*, 2019, **58**, 8145-8150.
12. R. Shi, D. Lv, Y. Chen, H. Wu, B. Liu, Q. Xia and Z. Li, Highly selective adsorption separation of light hydrocarbons with a porphyrinic zirconium metal-organic framework PCN-224, *Separation and Purification Technology*, 2018, **207**, 262-268.
13. S. Gao, C. G. Morris, Z. Lu, Y. Yan, H. G. Godfrey, C. Murray, C. C. Tang, K. M. Thomas, S. Yang and M. Schroder, Selective hysteretic sorption of light hydrocarbons in a flexible metal–organic framework material, *Chemistry of Materials*, 2016, **28**, 2331-2340.
14. Y. Huang, Z. Lin, H. Fu, F. Wang, M. Shen, X. Wang and R. Cao, Porous anionic indium-organic framework with enhanced gas and vapor adsorption and separation ability, *ChemSusChem*, 2014, **7**, 2647-2653.
15. Y. He, Z. Zhang, S. Xiang, F. R. Fronczek, R. Krishna and B. Chen, A robust doubly interpenetrated metal–organic framework constructed from a novel aromatic tricarboxylate for highly selective separation of small hydrocarbons, *Chem. Commun.*, 2012, **48**, 6493-6495.
16. G. Han, K. Wang, Y. Peng, Y. Zhang, H. Huang and C. Zhong, Enhancing Higher Hydrocarbons Capture for Natural Gas Upgrading by Tuning van der Waals Interactions in fcu-Type Zr-MOFs, *Industrial & Engineering Chemistry Research*, 2017, **56**, 14633-14641.
17. Y.-P. He, Y.-X. Tan and J. Zhang, Tuning a layer to a pillared-layer metal–organic framework for adsorption and separation of light hydrocarbons, *Chem. Commun.*, 2013, **49**, 11323-11325.
18. W. Liang, H. Xiao, D. Lv, J. Xiao and Z. Li, Novel asphalt-based carbon adsorbents with super-high adsorption capacity and excellent selectivity for separation for light hydrocarbons, *Sep. Purif. Technol.*, 2018, **190**, 60-67.
19. J. Gu, X. Sun, L. Kan, J. Qiao, G. Li and Y. Liu, Structural Regulation and Light Hydrocarbon Adsorption/Separation of Three Zirconium–Organic Frameworks Based on Different V-Shaped Ligands, *ACS Appl. Mater. Interfaces*, 2021, **13**, 41680-41687.
20. W. Fan, Y. Wang, Q. Zhang, A. Kirchon, Z. Xiao, L. Zhang, F. Dai, R. Wang and D. Sun, An Amino-Functionalized Metal-Organic Framework, Based on a Rare Ba_{12} $(COO)_{18}$ $(NO_3)_2$ Cluster, for Efficient C3/C2/C1 Separation and Preferential Catalytic Performance, *Chem-Eur J*, 2018, **24**, 2137-2143.
21. P. Huang, C. Chen, M. Wu, F. Jiang and M. Hong, An indium–organic framework for the efficient storage of light hydrocarbons and selective removal of organic dyes, *Dalton Transactions*, 2019, **48**, 5527-5533.
22. W. Fan, X. Wang, B. Xu, Y. Wang, D. Liu, M. Zhang, Y. Shang, F. Dai, L. Zhang and D. Sun, Amino-functionalized MOFs with high physicochemical stability for efficient gas storage/separation, dye adsorption and catalytic performance, *Journal of Materials Chemistry A*, 2018, **6**, 24486-24495.
23. C. X. Chen, S. P. Zheng, Z. W. Wei, C. C. Cao, H. P. Wang, D. Wang, J. J. Jiang, D. Fenske and C. Y. Su, A robust metal–organic framework combining open metal sites and polar groups for methane purification and CO_2/fluorocarbon capture, *Chem-Eur J*, 2017, **23**, 4060-4064.